JOC*Article*

The Three Corrugated Surfaces of 1,4-Divinyltetramethylene Diradical Intermediates and Their Connections to 1,2-Divinylcyclobutane, 4-Vinylcyclohexene, 1,5-Cyclooctadiene, and Two Butadienes

Pierluigi Caramella,*,† Paolo Quadrelli,† Lucio Toma,† Silvano Romano,‡ Kelli S. Khuong,§ Brian Northrop,§ and K. N. Houk*,§

Dipartimento di Chimica Organica, Università degli Studi di Pavia, Viale Taramelli 10, 27100, Pavia, Italy, Istituto Nazionale per la Fisica della Materia e Dipartimento di Fisica "A. Volta", Università degli Studi di Pavia, Via Bassi 6, 27100, Pavia, Italy, and Department of Chemistry and Biochemistry, University of California, Los Angeles, California 90095

pierluigi.caramella@unipv.it; houk@chem.ucla.edu.

Received January 31, 2005

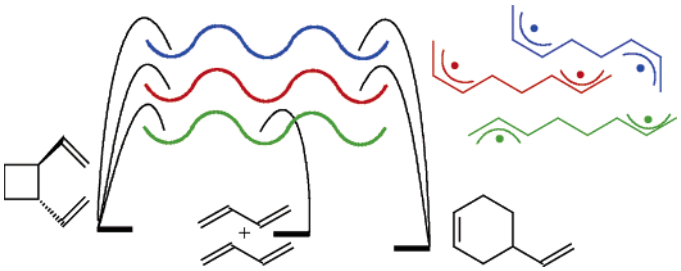

The three potential energy surfaces of the trans-trans, cis-trans, and cis-cis divinyltetramethylene diradicals have been located with DFT calculations at the BPW91/6-311+G** levels. The three surfaces account well for the experimental results reported for the thermolysis of optically active *trans*-1,2-divinylcyclobutane and optically active and deuterated 4-vinylcyclohexene. The surfaces account also for the outcome of the dimerization of butadiene and the thermolysis of *cis*,*cis*-1,5-cyclooctadiene. The three diradical intermediates are connected to the cyclization and dissociation products through conformations that are explored fully here.

The mechanism of the Diels−Alder (DA) reaction has attracted a huge number of investigations and the concerted mechanism has emerged[1] as the lowest energy mode of union of 4π and 2π addends in keeping with the orbital symmetry rules.[2] Only in special cases do two-step mechanisms compete or even predominate.[3] In this context the dimerization of butadiene BD **1** has attracted considerable attention since the major product (>85%) at 150−200 °C is the DA cycloadduct 4-vinylcyclohexene (VCH) **2** along with smaller but significant (5−10%) amounts[4] of the isomeric *trans*-1,2-divinylcyclobutane (DVCB) **t-3** and *cis*,*cis*-1,5-cyclooctadiene (COD) **4**, derived from the forbidden [2+2] and [4+4] modes of union, respectively (Scheme 1). The reaction provides an interesting prototypal case where concerted and diradical paths may compete. The diradical path should involve the *trans*,*trans*-1,4-divinyltetramethylene (DVT) diradicals **tt-5**, which should undergo the typical closure[5] to cyclobutanes, affording the trans DVCB **t-3** and the cis DVCB **c-3**. The latter is known[6] to undergo a rapid Cope rearrangement under the reaction conditions to COD **4**.

According to thermochemical estimates,[7] the cis,trans and cis,cis DVTs **ct-5** and **cc-5** lie at energies progressively higher than **tt-5** owing to the destabilization (ca.

† Dipartimento di Chimica Organica, Università degli Studi di Pavia.
‡ Istituto Nazionale per la Fisica della Materia e Dipartimento di Fisica "A. Volta", Università degli Studi di Pavia.
§ Department of Chemistry and Biochemistry, University of California.

(1) For an historical perspective, see: Houk, K. N.; Gonzalez, J.; Li, Y. *Acc. Chem. Res.* **1995**, *28*, 81−90.
(2) Woodward, R. B.; Hoffmann, R. *The Conservation of Orbital Symmetry*; Academic Press: New York, 1970.
(3) (a) Wassermann, A. *Diels−Alder Reactions*; Elsevier: Amsterdam, The Netherlands, 1965. (b) Sauer, J. *Angew. Chem.*, *Int. Ed. Engl.* **1967**, *6*, 16−33. (c) Sauer, J.; Sustmann, R. *Angew. Chem.*, *Int. Ed. Engl.* **1980**, *19*, 779−807. (d) Oppolzer, W. In *Comprehensive Organic Synthesis*; Paquette, L. A., Ed.; Pergamon Press: Oxford, UK, 1991; Vol. 5, pp 315−399.
(4) (a) Onishchenko, A. S. *Diene Synthesis*; Israel Program for Scientific Translation Ltd.: Jerusalem, Isreal, 1964; pp 592−597. (b) Reed, H. W. B. *J. Chem. Soc.* **1951**, 685−687.
(5) Schaumann, E.; Ketcham, R. *Angew. Chem.*, *Int. Ed. Engl.* **1982**, *21*, 225−247.
(6) Vogel, E. *Justus Liebigs Ann. Chem.* **1958**, *615*, 1−14.

10.1021/jo0501947 CCC: $30.25
Published on Web 03/19/2005

SCHEME 1

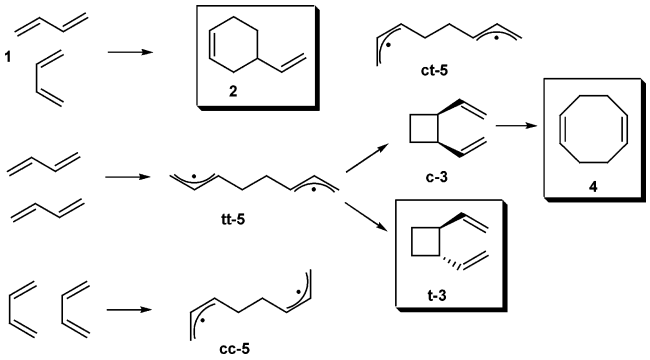

0.8−1.0 kcal/mol) of the *Z* substituted allyl radical. They are configurationally locked because of the (14 kcal/mol) allyl resonance, which offsets the geometrical isomerization of the allyl radical. The **ct** and **cc** DVTs could be formed by a 1,1′ coupling of a cisoid and a transoid butadiene moiety or through the coupling of two cisoid butadienes, respectively, and could afford all the dimers **2**−**4**. The DVT **ct-5** is directly related to the [2+2] and [4+2] dimers and only indirectly connected to the [4+4] dimer through the easy Cope rearrangement of DVCB **c-3**, while the DVT **cc-5** can afford directly all the dimers.

The DVTs **ct-5** and **cc-5** are somewhat redundant intermediates in the dimerization of butadiene in the sense that they are not strictly required to account for the products of the dimerization. Indeed the elegant studies by Stephenson and Klärner on the dimerization of *cis*,*cis*-1,4-dideuterio-1,3-butadiene[8] are consistent with the concerted formation of the DA [4+2] dimer **2** (through two concerted DA endo and exo pathways of similar importance) along with minor diradical pathways leading to *trans*-DVCB and COD. Thermochemical estimates[9] suggest the involvement of the DVT diradicals **tt-5** in the diradical pathways.

The DVTs **ct-5** and **cc-5** are, however, likely intermediates in the thermolysis of the dimers **2**, **t-3**, and **4**. While the cis DVCB **c-3** easily undergoes a Cope rearrangement to COD **4** at 120 °C, the trans isomer **t-3** rearranges more reluctantly. Hammond and DeBoer[10] reported in 1964 that thermolysis of DVCB **t-3** at 150−200 °C afforded mainly VCH **2** along with COD **4** and some butadiene (Scheme 2). Starting from optically active **t-3**, they found that the rate of racemization is only slightly faster than the rate of appearance of the rearranged products and that some of the optical activity is maintained in the VCH product. A decade later, Berson[11]

SCHEME 2

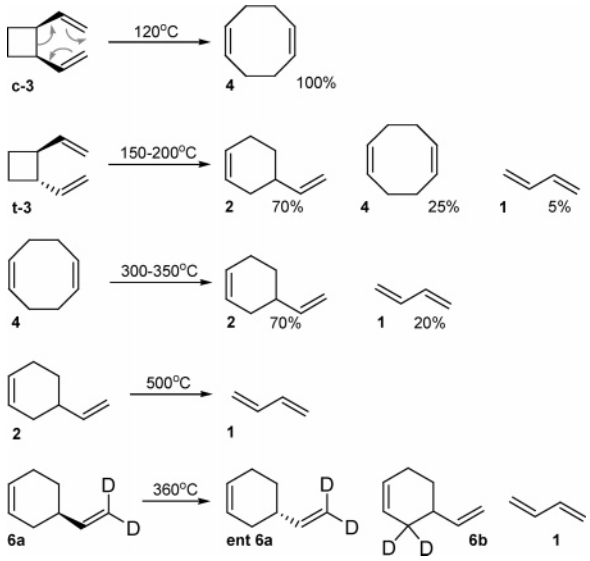

elegantly showed that the rearrangement takes place with predominant inversion of configuration at the migrating center, leading to a formal 1,3-sigmatropic shift that is suprafacial with inversion. The activation enthalpy of the racemization ($\Delta H^{\ddagger}$ = 36.3 kcal/mol) is, however, higher than that of the rearrangement (34.0 kcal/mol), while the activation entropies ($\Delta S^{\ddagger}$ = 4.6 and −1.2 eu, respectively) more than compensate for the enthalpic difference. These results imply the involvement of a chiral DVT **ct-5** in the rearrangement as well as the more stable chiral DVT **tt-5** having a somewhat reduced conformational flexibility and a sizable rotational barrier to reach a conformation that racemizes.

Srinivasan and Levi[12] investigated the thermolysis of COD **4**; this rearranges at 300−350 °C affording mainly the more stable VCH isomer **2** along with some butadiene. The most stable dimer is VCH **2**, which requires more stringent conditions (500 °C) to enter the retro-DA channel affording butadiene.[13] Doering et al.[7a] found that optically active **6a** undergoes racemization and deuterium exchange to **6b** at 360 °C with rates much faster than cycloreversion. Racemization ($\Delta H^{\ddagger}$ = 49.6 kcal/mol) is favored over deuterium exchange ($\Delta H^{\ddagger}$ = 52.1 kcal/mol), consistent with the involvement of a **ct** DVT in the racemization and the less stable **cc** DVT in the deuterium rearrangement.

In previous work[14] we have investigated the dimerization of butadiene using DFT methods at the B3LYP level with the 6-311+G** basis set. A concerted bis-pericyclic transition structure (TS) **7CN** and the pericyclic TS **7TX**

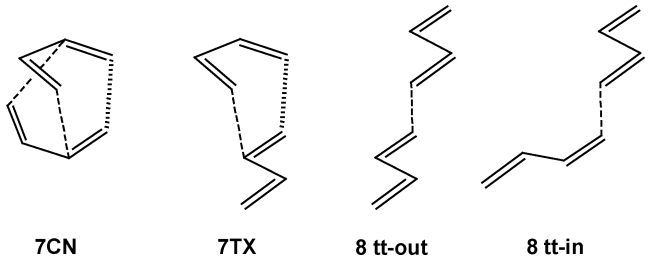

are the lowest transition states for the dimerization; they have identical energies, thus accounting for the lack of

(7) (a) Roth, W. R.; Staemmler, V.; Neumann, M.; Schmuck, C. *Liebigs Ann* **1995**, 1061−1118 and references therein. (b) Benson, S. W. *J. Chem. Phys.* **1967**, *46*, 4920−4926.

(8) (a) Stephenson, L. M.; Gemmer, R. V.; Current, S. *J. Am. Chem. Soc.* **1975**, *97*, 5909−5910. (b) Klärner, F. G.; Krawczyk, B.; Ruster, V.; Deiters, U. K. *J. Am. Chem. Soc.* **1994**, *116*, 7646−7657.

(9) (a) Doering, W. V. E.; Franck-Neumann, M.; Hasselmann, D.; Kaye, R. L. *J. Am. Chem. Soc.* **1972**, *94*, 3833−3844. (b) Li, Y.; Houk, K. N. *J. Am. Chem. Soc.* **1993**, *115*, 7478−7485. (c) Houk, K. N.; Li, Y.; Stohrer, J.; Raimondi, L.; Beno, B. R. *J. Chem. Soc., Faraday Trans.* **1994**, *90*, 1599−1604.

(10) (a) Hammond, G. S.; DeBoer, C. D. *J. Am. Chem. Soc.* **1964**, *86*, 899−902. (b) Trecker, D. J.; Henry, J. P. *J. Am. Chem. Soc.* **1964**, *86*, 902−905.

(11) (a) Berson, J. A.; Dervan, P. B. *J. Am. Chem. Soc.* **1973**, *95*, 267−270. (b) Berson, J. A.; Dervan, P. B.; Malherbe, R.; Jenkins, J. A. *J. Am. Chem. Soc.* **1976**, *98*, 5937−5968.

stereochemical preferences as observed experimentally by Stephenson and Klärner.[8] The two diradical forming TSs **8 tt-out** and **8 tt-in** lead to diradicals and have about the same energy as **7CN** and **7CX**. There are also TSs 2−3 kcal/mol higher involving cisoid dienes. The calculations account for the formation of all the dimers **1**−**4**, but TS **8 tt-in** and **8 tt-out** are too low in energy.

More recently we used the BPW91 functional recommended by Davidson[15] for comparisons of pericyclic and diradical-forming pathways. This functional performs well in the dimerization of butadiene, giving an evaluation of the concerted and diradical-forming TSs that is closer to the experimental data. We have therefore investigated more thoroughly the potential surface of the DVTs at the BPW91 level with the 6-31G* and 6-311+G** basis. We report here a study of the three potential surfaces of the **tt**, **ct**, and **cc** DVTs and their connections to the various butadiene dimers. The results offer a unifying picture of all the experimental results and account for the puzzling activation data.

Computational Methods

Geometries for all the stationary structures have been optimized at the BPW91 level by using the standard 6-31G* and 6-311+G** basis sets. The calculations were performed with the Gaussian 98 program.[16] Diradical and transition states leading to diradicals were treated with the unrestricted procedure, involving HOMO−LUMO mixing in the initial guess leading to unrestricted wave functions. All minima and transition states were characterized by their vibrational frequencies and all the reported thermodynamic data are given at 298.15 K from unscaled vibrational frequencies in the harmonic approximation. Intrinsic Reaction Coordinate (IRC) calculations starting at the saddle points were carried out to check the connections between the transition structures and the reactants and products.

Results

The DVT Diradicals 5. The DVT diradicals **tt-5** can undergo conformational changes by rotation about the allylic bond (α and α′) and the central C−C bond (β) as shown in **9**.

9

10

The torsional potential about the allylic bonds is 3-fold as shown for the simpler cases of *E* and *Z* 1-penten-3-yl radicals **10** which are displayed in Figure 1. The shape of the potential of the *E* pentenyl radical is similar to the familiar potential of 1-butene but the barriers are significantly lower in keeping with the known[17] stereochemical lability of radical centers. In the case of the *Z*-pentenyl radical the potential is still qualitatively similar but the A(1.3) strain raises the energies at low torsional angles and reduces remarkably the 180° barrier, too. In all cases the lowest barrier for the allyl (or vinyl) rotation is the antiperiplanar 180° barrier involving a methyl/hydrogen eclipsing and sketched in formulas for the pentenyl radicals.

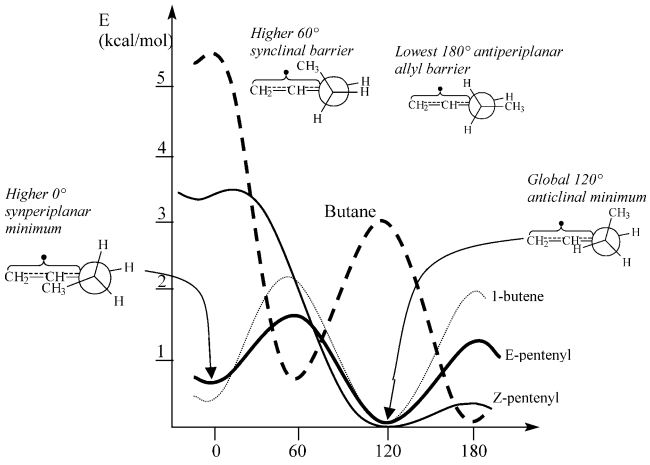

FIGURE 1. Torsional potential of the *E* and *Z* pentenyl radicals, 1-butene (dots), and butane (dashed line). The BPW91/6-31G* electronic energies are displayed. Formulas refer to the *E*-pentenyl profile.

Also shown in Figure 1 is the familiar torsional potential of butane about the C_2-C_3 bond as a model for the β torsion. The butane 120° barrier is higher (3.2 kcal/mol) than the allylic barriers, while the 0° barrier due to the methyl/methyl eclipsing stands alone as the highest barrier (5.6 kcal/mol).

Owing to the three V_3 potentials, the DVT diradicals **tt-5** should have a maximum of 27 conformations; the total number is reduced by symmetry or enantiomerism. This leaves 10 possible conformations of different energy, which are displayed in Figure 2 along with their relative BPW91/6-311+G** energies.

Conformations about the central bond are denoted by A (anti, β near 180°) or G and G− (gauche, β near 60° or −60°, respectively) and conformations about the allylic bonds are denoted as a and a− (anticlinal, α near 120° or −120°, respectively) or s (syn, α near 0°) starting from the allylic bond on the left. As expected, the A conformers involving two anti allyl moieties are the most stable ones while conformers involving syn allyl moieties lie at

(12) Srinivasan, R.; Levi, A. A. *J. Am. Chem. Soc.* **1964**, *86*, 3756−3759.
(13) (a) Duncan, N. E.; Janz, G. J. *J. Chem. Phys.* **1952**, 1644−1645. (b) Tsang, W. *J. Chem. Phys.* **1965**, *42*, 1805−1809.
(14) (a) Quadrelli, P.; Romano, S.; Toma, L.; Caramella, P. *Tetrahedron Lett.* **2002**, *43*, 8785−8789. See also: (b) Caramella, P.; Quadrelli, P.; Toma, L. *J. Am. Chem. Soc.* **2002**, *124*, 1130−1131. (c) Quadrelli, P.; Romano, S.; Toma, L.; Caramella, P. *J. Org. Chem.* **2003**, *68*, 6035−6038.
(15) (a) Staroverov, V. N.; Davidson, E. R. *J. Am. Chem. Soc.* **2000**, *122*, 7377−7385. (b) Staroverov, V. N.; Davidson, E. R. *J. Mol. Struct.* (*THEOCHEM*) **2001**, *573*, 81−89.
(16) Frisch, M. J.; Trucks, G. W.; Schlegel, H. B.; Scuseria, G. E.; Robb, M. A.; Cheeseman, J. R.; Zakrzewski, V. G.; Montgomery, J. A., Jr.; Stratmann, R. E.; Burant, J. C.; Dapprich, S.; Millam, J. M.; Daniels, A. D.; Kudin, K. N.; Strain, M. C.; Farkas, O.; Tomasi, J.; Barone, V.; Cossi, M.; Cammi, R.; Mennucci, B.; Pomelli, C.; Adamo, C.; Clifford, S.; Ochterski, J.; Petersson, G. A.; Ayala, P. Y.; Cui, Q.; Morokuma, K.; Malick, D. K.; Rabuck, A. D.; Raghavachari, K.; Foresman, J. B.; Cioslowski, J.; Ortiz, J. V.; Stefanov, B. B.; Liu, G.; Liashenko, A.; Piskorz, P.; Komaromi, I.; Gomperts, R.; Martin, R. L.; Fox, D. J.; Keith, T.; Al-Laham, M. A.; Peng, C. Y.; Nanayakkara, A.; Gonzalez, C.; Challacombe, M.; Gill, P. M. W.; Johnson, B. G.; Chen, W.; Wong, M. W.; Andres, J. L.; Head-Gordon, M.; Replogle, E. S.; Pople, J. A. *Gaussian 98*, Revision A.9; Gaussian, Inc.: Pittsburgh, PA, 1998.
(17) (a) Fischer, H. *Free Radicals*; Kochi, J. K., Ed.; Wiley: New York, Vol. 2, 1973; pp 435−491. (b) Jasperse, C. P.; Curran, D. P.; Fevig, T. L. *Chem. Rev.* **1991**, *91*, 1237−1286.

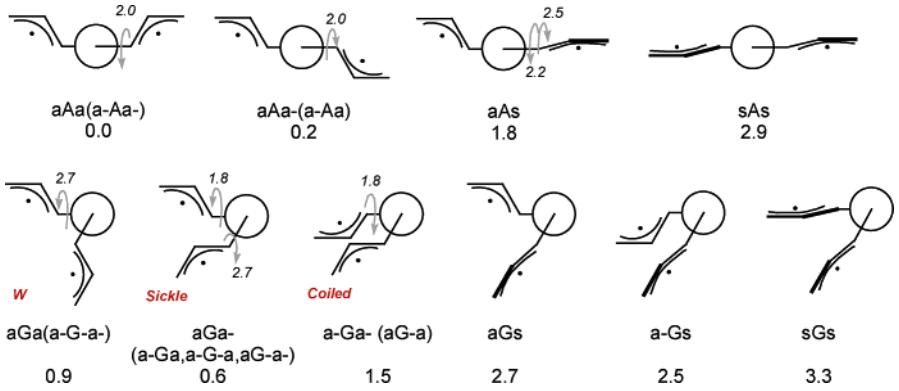

FIGURE 2. The BPW91/6-311+G** conformers of DVT **tt-5**. Numbers below the symbols specify the energy of the conformers (in kcal/mol) relative to the lowest aAa **tt-5** conformer. Arrows indicate the rotation toward the antiperiplanar allylic barriers or synclinal barriers in the case of syn conformers. Numbers near the arrows are the energies of the rotation TSs. Conformational labels in parentheses specify equivalent conformations discussed in the text or shown in the tables.

significantly higher energy. Among the G conformers the sickle aGa− (0.6 kcal/mol) is slightly more stable than the W-shaped aGa (0.9) while the coiled a-Ga− is the highest in energy (1.5). For the sake of clarity the labels W, sickle, and coiled will be extensively used to differenciate the G conformers. The allylic barriers of the aAa and aAa− conformers are moderate (1.8−2.0 kcal/mol) and change somewhat in the G conformers.

The conformers of the **ct** and **cc** diradicals are similar with the **tt** ones and are shown in the Supporting Information. Two conformers, the coiled a-Ga− **ct-5** and the sickle aGa− **cc-5** are, however, unstable to cyclization to VCH (vide infra). The coiled **ct-5** conformer could be located at the UBPW/6-31G* level but the shallow minimum disappears at the 6-311+G** level. The sickle **cc-5** is inherently unstable and its energy was estimated with constrained optimizations.

The electronic energies, enthalpies, entropies, and free energies of the relevant conformers of the DVT diradicals **5** are given in the Supporting Information along with the lowest antiperiplanar allylic barriers. The thermodynamic data are not statistically corrected[18] as they should be for the purpose of determining the equilibrium conformer distributions. The presence of the *Z*-allyl moiety raises the conformer energies in the **ct** and **cc** series by about 1 and 2 kcal/mol, respectively and halves the allylic barriers of the *Z*-allylic moieties (about 1 kcal/mol) with respect to the *E* ones, in keeping with thermochemical estimates[9] and the model calculations of Figure 1. Noteworthy on going from the electronic energies to the enthalpies the relative energies of the rotation TSs lower sizably, i.e., the enthalpic surface smooths out. Entropies more than compensate for the enthalpic effect and the free energy surfaces of the diradicals look like the electronic ones. In the figures the electronic energies are used for the plots, which correspond more closely to the free energy landscape, unless otherwise reported.

The barriers about the central bond of the DVT diradicals are much larger and more important in determining the chemistry of these intermediates. The three "butane" A/G (dihedral 120°) barriers **11a**−**c** and the two G/G− barriers (dihedral = 0°) **12a**,**b** for the rotations of **tt-5** are shown in Figure 3. The energy data

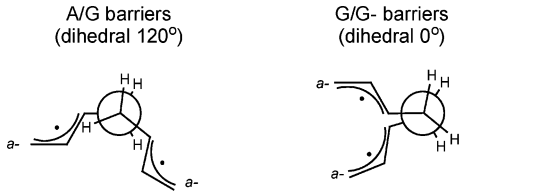

11a a-A/Ga- 2.5
11b aA/Ga- (=a-A/Ga) 2.8
11c aA/Ga 3.6

12a a-G/G-a- (= aG/G-a) 5.2
12b aG/G-a- (=a-G/G-a) 5.7

FIGURE 3. The BPW91/6-311G* "butane" barriers of DVT **tt-5**. Formulas refer to **11a** and **12a**. Numbers near the symbols specify the energy of the rotation TSs relative to the lowest **tt-5** aAa conformer.

of the "butane" barriers are given in the Supporting Information. In general A/G barriers range from 2.4 to 3.6 while G/G− barriers range around 5−5.5 kcal/mol, in good agreement with expectations based on the butane model.

The Thermolysis of *trans*- and *cis*-1,2-Divinylcyclobutanes. The relevant points on the potential energy surface for the ring opening of DVCB have been located. Structures **t-3** and **c-3** lead to the diradicals **5** by homolysis of the labile cyclobutane bonds. Moreover the DVCB **c-3** are connected through the lowest[19] Cope TS to COD **4**, which adopts the lowest twist-boat conformations,[20] and higher Cope TSs[19] (not shown) connect **c-3** to cis,trans and trans,trans 1,5-cyclooctadienes. The energy data of the TSs, DVCB reactants, and products are given in Table 1, and the electronic energies relative to the aAa **tt-5** diradical are displayed in Figure 4 along with the formulas.

The lowest conformations of DVCB **t-3** and **c-3** are sketched in **13** and **14**. The vinyl groups occupy the most

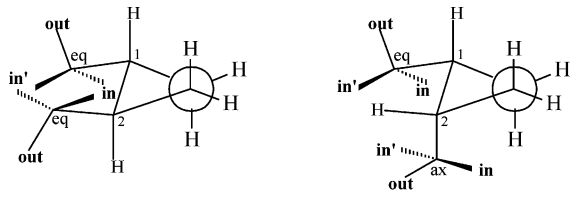

13 **14**

favorable diequatorial, **13**, or axial and equatorial, **14**, conformations. The distal vinylic carbons occupy the **out**

(18) Eliel, E. L.; Wilen, S. H. *Stereochemistry of Organic Compounds*; John Wiley & Sons: New York: 1994; pp 601−602.

TABLE 1. BPW91/6-311+G Electronic Energies ΔE_e, Enthalpies, Free Energies (kcal/mol)[a] and Entropies (eu),[a] Breaking C···C Bonds Lengths (Å) of the TSs, DVCB Conformers t-3 and c-3, and Products in the Thermolysis of 1,2-Divinylcyclobutanes t-3 and c-3 Relative to Trans DVCB t-3[b,c]**

compd		ΔE_e	ΔH	ΔS	ΔG	C···C
			transition structures			
15 diequatorial	out-out	30.9 (2.4)	28.2 (2.0)	1.2 (−5.6)	27.8 (3.6)	2.59
	in-out	31.3 (2.8)	28.7 (2.5)	0.7 (−6.1)	28.4 (4.2)	2.59
	in-in	31.6 (3.1)	29.1 (2.9)	0.2 (−6.6)	29.0 (4.8)	2.60
16 diaxial	out-out	34.9 (6.4)	32.1 (5.9)	3.6 (−3.2)	31.0 (6.8)	2.54
	in-out	34.9 (6.4)	32.3 (6.1)	1.9 (−4.9)	31.7 (7.5)	2.55
	in-in	35.0 (6.5)	32.5 (6.3)	0.0 (−6.8)	32.4 (8.2)	2.56
17 axial-equat.	out-out	33.2 (4.7)	30.4 (4.2)	2.6 (−4.2)	29.7 (5.5)	2.58
	out-in	33.6 (5.1)	30.9 (4.7)	1.9 (−4.9)	30.4 (6.2)	2.60
	in-out	33.1 (4.6)	30.5 (4.3)	0.8 (−6.0)	30.2 (6.0)	2.57
	in-in	33.0 (4.5)	30.5 (4.3)	0.2 (−6.6)	30.5 (6.3)	2.66
Cope **18**		22.8 (−5.7)	21.8 (−4.4)	-6.0 (−12.8)	23.6 (−0.6)	2.16 (2.43)[e]
			1,2-divinylcyclobutanes			
t-3	out-out	≡0.0[b] (−28.5)	≡0.0 (−26.2)	≡0.0 (−6.8)	≡0.0 (−24.2)	
	in-out	0.3 (−28.2)	0.4 (−25.8)	−1.0 (−7.8)	0.7 (−23.5)	
	in-in	1.3 (−27.2)	1.4 (−24.8)	−0.7 (−7.5)	1.6 (−22.6)	
t-3AX	out-out	[2.4][d]				
	in-out	[3.1][d]				
	in-in	[3.2][d]				
c-3	out-out	2.4 (−26.1)	2.4 (−23.8)	−0.5 (−7.3)	2.6 (−21.6)	
	in-out	2.8 (−25.7)	2.9 (−23.3)	−0.8 (−7.6)	3.2 (−21.0)	
	out-in	2.6 (−25.9)	2.5 (−23.7)	−0.8 (−7.6)	2.8 (−21.4)	
	in-in	3.9 (−24.6)	3.9 (−22.3)	−0.4 (−7.2)	4.0 (−20.2)	
			products			
COD 4		−15.5 (−44.0)	−14.0 (−40.2)	−6.6 (−13.4)	−12.1 (−36.3)	
tt-5	aAa	28.5 (≡0.0)	26.2 (≡0.0)	6.8 (≡0.0)	24.2 (≡0.0)	
ct-5	aAa−	29.4 (0.9)	27.3 (1.1)	6.1 (−0.7)	25.5 (1.3)	
cc-5	aAa−	30.3 (1.8)	28.5 (2.3)	7.7 (0.9)	26.2 (2.0)	

[a] Thermodynamic values at 298.15 K from unscaled vibrational frequencies in the harmonic approximation. [b] DVCB **t-3 out out** −312.032068 hartrees, correction to enthalpy $\delta H = 113.71$, $S = 91.76$. [c] Numbers in parentheses are energies and thermodynamic data relative to the lowest energy conformer of diradical **tt-5** aAa. [d] BPW91/6-31G* electronic energies. [e] Forming COD bond.

positions, eclipsing the CH bonds. Slightly less favorable options are the **in** positions, with eclipsing of the lateral C1−C4 or C2−C3 bonds. The **in′** positions are even less favorable since they involve eclipsing with the central C1−C2 bond and crowding with the vicinal substituents. The lowest diequatorial conformations of **t-3** are shown on the top left of Figure 4 while the related axial−equatorial conformations of **c-3** are on the top right. In the **in/out** conformational labels the substituents at C1 in **13** and **14** are given first and those at C2 second.

The lowest TSs for the diradical-forming ring opening of DVCB **t-3** are the diequatorial TSs **15 out-out**, **in-out**. and **in-in**, which connect the corresponding diequatorial **t-3** conformers to the coiled G conformers of **tt**, **ct**, and **cc** DVT **5**, respectively. The diaxial TSs **16** lie at sizably higher energies and connect the **t-3AX** conformers to the W shaped G conformers. Between are located the TSs **17** of the ring opening of the cis DVCB conformers **c-3**. These TSs, **17**, connect them to the sickle G diradicals **5**, while the **in-in c-3** conformer is also connected to COD **4** through the low-lying Cope TS **18**.

In the ring opening to the diradicals **5**, the same energy ordering of the ground state conformations is maintained. The parallelism derives from the fact that vinyl substituents in the more stable equatorial location of DVCBs have the π orbitals properly oriented to assist the cleavage of the 1,2 bond, while axial substituents encounter substantial strain in the ground state and poorer overlap of π orbitals with the breaking bond in the cleavage. In the ring cleavage TSs, the C1−C2 bonds lengthen to 2.53−2.60 Å and the cyclobutane C1−C2−C3−C4 dihedral angles increase to 30−40°. The equatorial vinyl substituents (the incipient allylic radicals) and the geminal hydrogens then rotate in order to achieve the most favorable conformations of the diradicals. The vinyl groups eclipse the boldface vicinal hydrogens as indicated in **19**, giving the structure an uncanny conrotatory appearance. Axial vinyl substituents maintain the same conrotatory look but require more reorganization as shown in the Newman projection **20**. Here the long

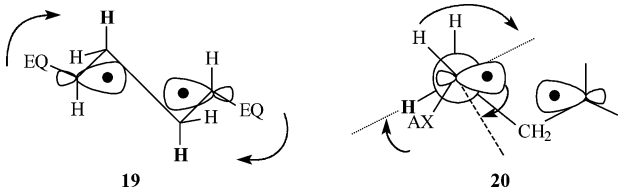

19 **20**

dotted line indicates the final eclipsed location of the radical substituents (AX and the geminal H) and the orthogonal dashed line indicates the final location of the depyramidalized singly occupied orbital. The axial vinyl rotates to eclipse the boldface vicinal hydrogen, while the geminal H and the singly occupied orbital also must rotate and cannot avoid unfavorable eclipsings.

Connections of Diradicals 5 to VCH and COD. The coiled and the sickle conformers of the DVTs **ct-5** and

(19) (a) Zora, M.; Özkan, I. *J. Mol. Struct.* (*THEOCHEM*) **2003**, *625*, 251−256. (b) Özkan, I.; Zora, M. *J. Org. Chem.* **2003**, *68*, 9635−9642. See also: (c) Zora, M. *J. Org. Chem.* **2004**, *69*, 857−862.

(20) (a) Allinger, N. L.; Sprague, J. T. *J. Am. Chem. Soc.* **1972**, *94*, 5734−5747. (b) Shimizu, T.; Iwata, K.; Kamigata, N.; Ikuta, S. *J. Chem. Res.* (*S*) **1994**, 436−437.

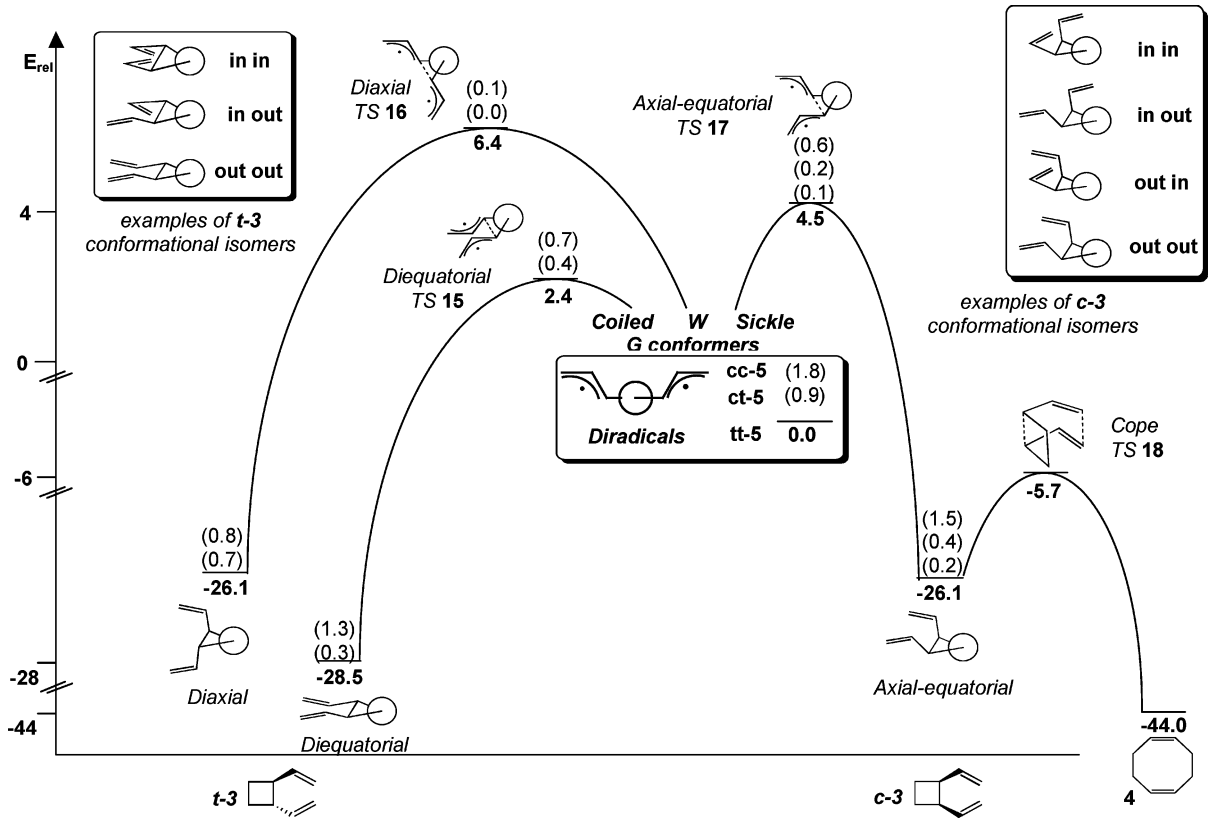

FIGURE 4. Transition structures, DVCB conformers, and products in the thermolysis of DVCB. Numbers near the levels are electronic energies (in kcal/mol) relative to lowest aAa **tt-5** conformer. Numbers in parentheses specify the energetic increase of other conformers above the given level. Numbers in the box of diradicals **5** refer to the more stable A conformers of the **tt-5**, **ct-5**, and **cc-5** diradicals.

cc-5 are flexible intermediates that cyclize easily affording VCH **2**. These diradicals have very small or no cyclization barriers on the electronic surface. Figure 5 summarizes the conformational switch of the **ct-5** and **cc-5** G diradicals through the allyl rotations and their main connections to DVCB **t-3**, VCH **2**, and COD **4**. The energetic data are gathered in Table 2.

In the **ct-5** case, the W-shaped and the sickle "out" conformers have the *Z* allylic moieties directed away from the *E* allylic ones. These possess stable minima, while the coiled and the sickle "in" conformers have the *Z* allylic moieties directed toward the *E* ones and have no (**tN**) or a quite small (**tX**) barrier for cyclization to VCH **2**. TS **21tN** could be located at the 6-31G* level but the TS disappears at the 6-311+G** level leaving on the electronic surface a smooth descending path from the coiled **ct-5** to VCH **2**. The shapes of the structures involved in the ring closure to VCH, TSs **21tN**, and **tX** are reminiscent of the related DA TSs from which they differ by the presence of a C−C bond and a long (3.2−3.3 Å) forming bond between the addends.

In the **cc-5** case the W conformer possesses a stable minimum. The coiled conformer displays a 1 kcal/mol barrier, which serves as the cyclization TS **21 cN**. This rather floppy and symmetrical TS resembles the VCH Cope TS **22** with the two allylic moieties far apart. This leads to a diradical species that smoothly collapses to the VCH Cope TS **22** and then forms VCH **2**. The sickle conformer is inherently unstable to cyclization and a smoothly descending path connects the flat plateau of the unstable sickle conformer to VCH **2**.

Attempts to locate paths between the diradicals **5** and COD involving a 4,4′ coupling led to the set of four TSs **17** where the more favorable cyclobutane 2,2′ couplings take place. Only in a few cases could high-lying TSs be located, such as the chair TS **23** connecting the coiled **cc-5** to the twist-boat COD **4** through its less stable[20] chair conformer, labeled as COD **4b** in Table 2. The most favorable connection of diradicals **5** to COD **4** is then indirect and involves cyclizations of the **tt**, **ct**, and **cc-5** sickle conformers to cis DVCB **c-3** through the set of four TSs **17** followed by the easy Cope rearrangement **18** of **c-3** to COD.

Connections of Diradicals 5 to Butadiene. The anti conformers of the DVT diradicals **5** are connected to butadiene through the diradical TSs **8** as shown in Figure 6. This figure also shows the DA cycloaddition TSs **7** and the concerted Cope TS **22** of the VCH interconversion. The energy data are gathered in Table 3. The ordering of the TSs in Figure 6 is significantly different from that already obtained with B3LYP/6-311+G** calculations.[14] The BPW91 functional improves remarkably the energetic description of these reactions giving a more balanced treatment of the diradical and concerted paths that is closer to the experimental results. The BPW91 functional raises the energy of the diradicals **5** and, to a lesser extent, the diradical-forming TSs **8**, with respect to the concerted asynchronous cycloaddition TSs

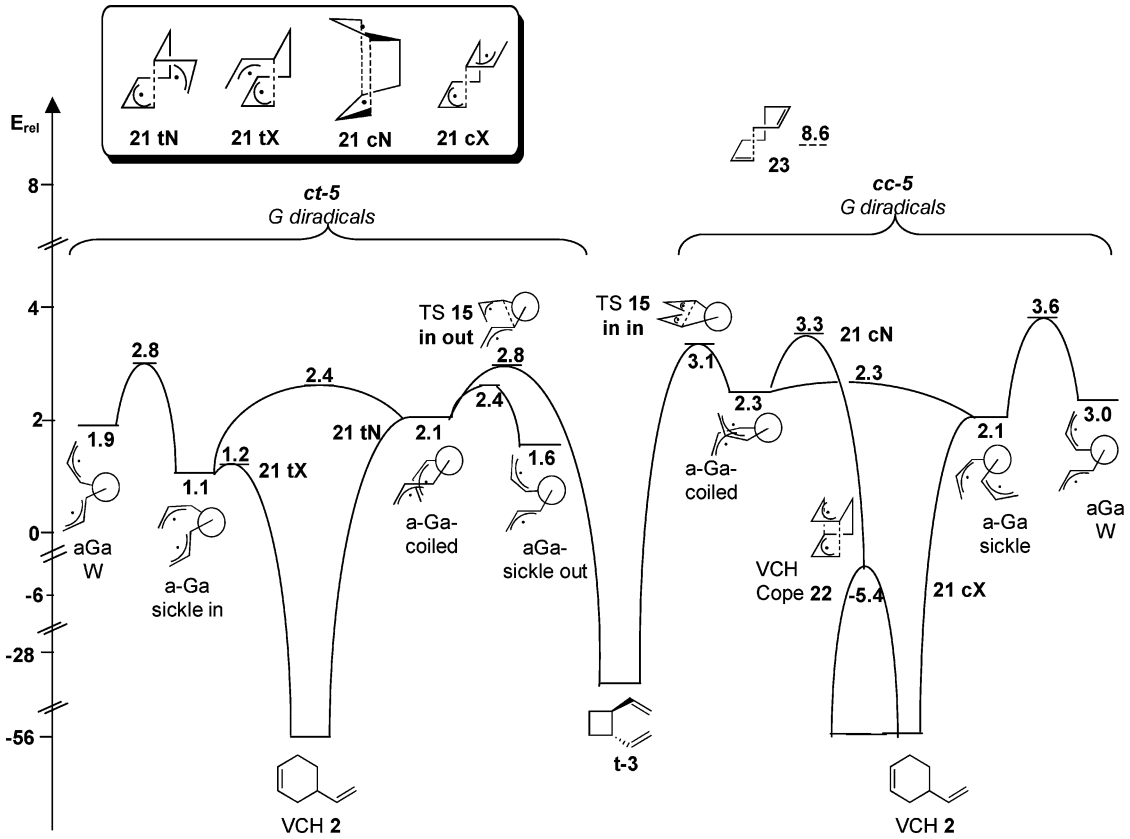

FIGURE 5. Connections of the G conformers of the DVTs **ct-5** and **cc-5** to VCH **2** through the structures **21 tN**, **tX**, **cN**, **cX**, and **22**. The coiled **cc-5** diradical is also directly linked to COD **4** through a high-lying TS **23**.

TABLE 2. BPW91/6-311+G Electronic Energies ΔE_e, Enthalpies, Free Energies (kcal/mol), and Entropies (eu)[a] of the TSs Connecting the Diradicals to VCH and COD Relative to the Lowest Diradical tt-5 aAa**

compd	ΔE_e	ΔH	ΔS	ΔG
	transition structures			
21tN	(2.0)[b]	(1.6)[b]	(−6.7)[b]	(3.6)[b]
21tX	1.2	0.9	−7.2	3.0
21cN	3.3	2.8	−5.5	4.4
21cX	c			
VCH Cope **22**	−5.4	−4.2	−15.4	0.4
23	8.2	7.9	−9.3	10.7
	products			
COD **4**	−44.0	−40.2	−13.4	−36.3
COD **4b**	−41.7	−38.0	−12.8	−34.2
VCH **2**	−50.3	−47.1	−11.6	−43.7

[a] Thermodynamic values at 298.15 K from unscaled vibrational frequencies in the harmonic approximation. [b] BPW91/6-311+G**// 6-31G* energies and 6-31G* thermodynamics. [c] Smooth descent from the flat plateau of the sickle **cc-5** conformer to VCH **2**.

7. This leaves the lowest DVT diradicals **tt-5** 3 kcal/mol below the diradical forming TSs **8**, accounting for the occurrence of small amounts of butadiene in the thermolysis of DVCB, COD, and VCH. The B3LYP location of the lowest DVT diradicals at 7 kcal/mol[14] below the diradical forming TSs **8** is not consistent with the experimentally observed formation of butadiene in the thermolyses of the butadiene dimers. The moderate increase of the energy of the diradical forming TSs **8** places them 1 kcal/mol above the lowest cycloaddition TS **7**, in agreement with the experimental evidence for concerted cycloaddition.[8] Entropy effects reverse however the balance and on the free energy surface TSs **8** stay 1 kcal/mol below the lowest TSs **7**. As outlined in the later discussion, the diradical forming steps are however reversible, thus reconciling experimental and computational results.

Attempts to locate the gauche diradical forming TSs **24** analogous to anti **8** and involving a gauche arrangement about the forming bond have been made at the BPW91/6-31G* level. A few of the gauche TSs could be located and are shown in Figure 7. The numbers specify electronic energies above the lowest TS **8**. A gauche approach of the two transoid butadienes is less favorable by 1.9 kcal/mol than the anti approach of TS **8**. The gauche approach becomes even less favorable in the **ct** and **cc** cases.

Discussion

The tt Surface: Hindered Racemization of DVCB and Reversibility of Butadiene 1,1′-Couplings. Scheme 3 shows the many conformations of the trans,-trans diradical that can be formed by homolysis of the labile bond of DVCBs or by union of two trans butadienes. The computed barriers for interconversions are given as electronic energies relative to aAa **tt-5** or, in parentheses, free energies at room temperature. More details are shown in Figure B in the Supporting Information. The labels *R* and *S* near the radical centers refer to the stereochemistry of DVCB coupling to the front allyl and allow deductions about racemization paths starting from chiral trans DVCB. The free energy profile is also summarized in Figure 8.

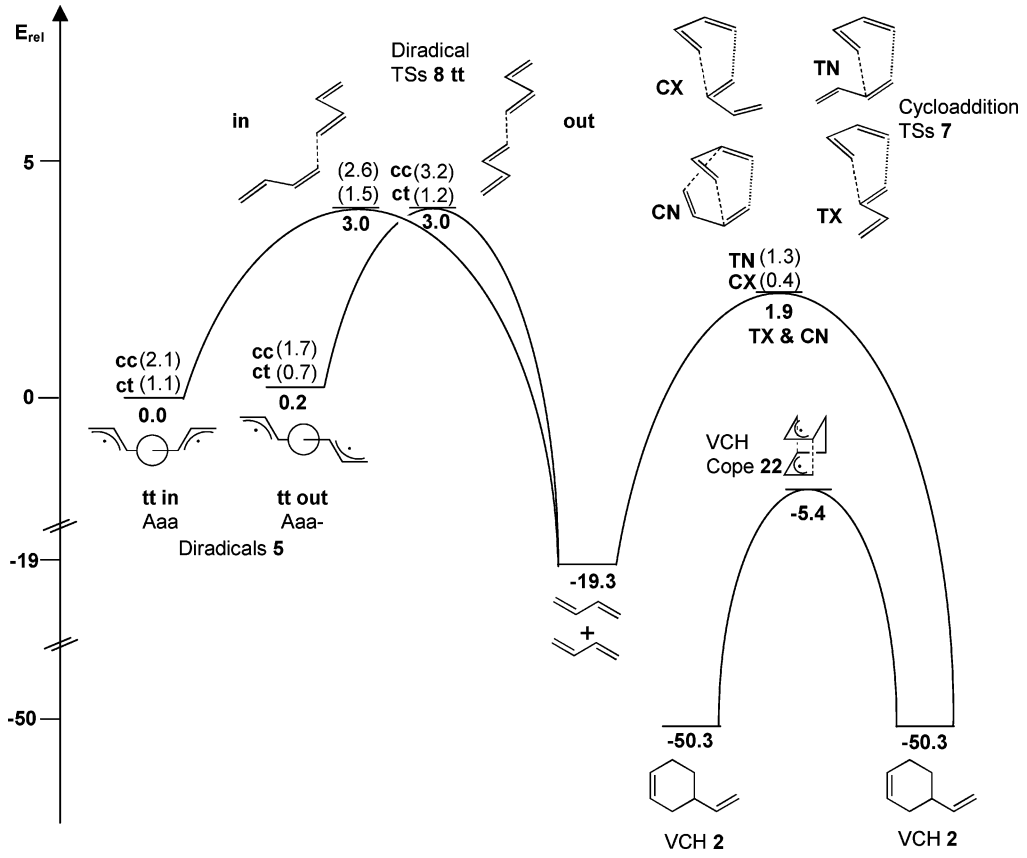

FIGURE 6. The BPW91/6−3111+G** transition structures, diradical intermediates, and DA cycloadducts in the butadiene dimerization. Numbers near levels are electronic energies (in kcal/mol) relative to diradical aAa **tt-5**. Numbers in parentheses specify the energetic increase of other stereoisomers above the given level.

TABLE 3. BPW91/6-311+G Electronic Energies ΔE_e Relative to the Reactants (kcal/mol), Enthalpies, Free Energies (kcal/mol), and Entropies (eu)[a] of the TSs, Diradical Species, and Cycloadduct in the Dimerization of Butadiene.[b,c]**

compd		ΔE_e	ΔH	ΔS	ΔG
		transition structures			
7CN		21.2 (1.9)	22.6 (2.1)	−28.7 (−6.9)	31.2 (4.2)
7CX		21.6 (2.3)	23.1 (2.6)	−28.1 (−6.3)	31.4 (4.4)
7TN		22.5 (3.2)	23.8 (3.3)	−28.2 (−6.4)	32.2 (5.2)
7TX		21.2 (1.9)	22.5 (2.0)	−27.6 (−5.8)	30.7 (3.7)
tt-8	**in**	22.3 (3.0)	23.1 (2.6)	−23.8 (−2.0)	30.2 (3.2)
tt-8	**out**	22.3 (3.0)	23.1 (2.6)	−23.6 (−1.8)	30.2 (3.2)
ct-8	**in**	23.8 (4.5)	24.8 (4.3)	−23.7 (−1.4)	31.8 (4.8)
ct-8	**out**	23.5 (4.2)	24.5 (4.0)	−24.3 (−2.5)	31.7 (4.7)
cc-8	**in**	24.9 (5.6)	26.3 (5.8)	−26.5 (−4.7)	34.2 (7.2)
cc-8	**out**	25.5 (6.2)	26.5 (6.0)	−22.7 (−0.9)	33.3 (6.3)
		adducts			
tt-5	aAa	19.3 (≡0.0)	20.5 (≡0.0)	-21.8 (≡0.0)	27.0 (≡0.0)
tt-5	aAa−	19.5 (0.2)	20.8 (0.3)	−21.2 (0.6)	27.1 (0.1)
ct-5	aAa	20.3 (1.0)	21.7 (1.2)	−20.7 (1.1)	27.9 (0.9)
ct-5	aAa−	20.2 (0.9)	21.6 (1.1)	−22.5 (−0.7)	28.3 (1.3)
cc-5	aAa	21.4 (2.1)	22.9 (2.4)	−19.9 (1.9)	28.8 (1.8)
cc-5	aAa−	21.2 (1.9)	22.7 (2.2)	−20.9 (0.9)	29.0 (2.0)
VCH Cope **22**		13.9 (−5.4)	16.3 (−4.2)	−37.2 (−15.4)	27.4 (0.4)
VCH **2**		−31.0 (−50.3)	−26.6 (−47.1)	−33.4 (−11.6)	−16.7 (−43.7)
butadiene	× 2	≡0.0 (−19.3)	≡0.0 (−20.5)	≡0.0 (21.8)	≡0.0 (−27.0)

[a] Thermodynamic values at 298.15 K from unscaled vibrational frequencies in the harmonic approximation. [b] *s-trans*-Butadiene, −156.008708 hartrees, correction to enthalpy $\delta H = 55.42$, $S = 66.43$; *s-cis*-butadiene, $\Delta E_e = 3.61$. [c] Numbers in parentheses are energies and thermodynamic data relative to the lowest diradical **tt-5** aAa.

The most striking feature of the surface is the comparable height of the electronic barriers (2.4−3 kcal/mol) of cyclizations of the coiled G conformers to tDVCB, cleavages of the A conformers to butadienes, and A/G conformational switches of the diradicals while other interconversions are less favorable. The free energy barriers (3.2−4.1 kcal/mol) follow the same trend and are somewhat raised mainly because of entropy effects which

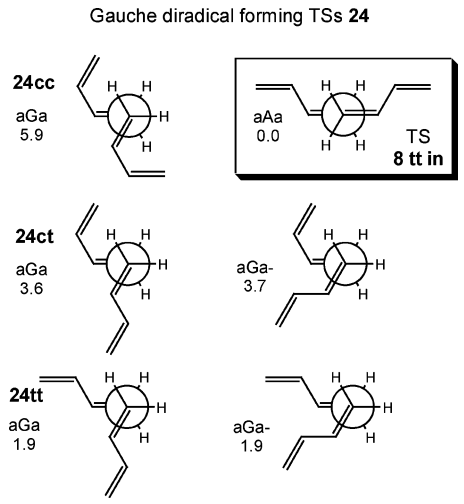

FIGURE 7. Diradical forming TSs **24** for the gauche approach of transoid and cisoid butadienes. Labels are the same as those used to label the corresponding diradical conformers. Numbers near the labels are BPW91/6-31G* electronic energies relative to the lowest TS **8 tt-in** shown in the inset.

reflect the higher order of the TSs. The comparable barriers imply the reversibility of either the butadiene 1,1′ couplings (TSs **8**) or the selective tDVCB opening to the coiled conformer (TS **15 out-out**).

The reversibility of the butadiene 1,1′ coupling is at variance with the common assumption of an irreversible entry into the flat tetramethylene manifold (the twixtyl or caldera)[21] where "fast internal rotations interrelate the various conformations, and slower collapses to trans- and cis-1,2-divinyl cyclobutane take place"[21a] and accommodate the rather disturbing result of the calculations (Table 3), which place the free energies of the diradical forming TSs **8 tt** 1 kcal/mol below the concerted cycloaddition TSs **7CN** and **7CX**. In the case of consecutive first-step reversible reactions the rate depends on the partitioning of the intermediate according to the familiar steady-state expressions:[22]

$$\mathrm{nA} \underset{k_{-1}}{\overset{k_1}{\rightleftharpoons}} \mathrm{B} \xrightarrow{k_2} \mathrm{C} \qquad (n = 1, 2)$$

$$k_{\mathrm{obs}} = k_1 \frac{k_2}{k_2 + k_{-1}} \tag{1}$$

The reaction rate decreases with respect to the entry rate k_1 causing an increase of the free energy of the path and a related decrease of the entropy by $R \ln[(k_2 + k_{-1})/k_2]$. In the simple case of identical rates of return and product forming step the reaction rate is halved, $\Delta G^{\ddagger}$ increases by $RT \ln 2$, and $\Delta S^{\ddagger}$ decreases by $R \ln 2$, i.e., 0.6 kcal/mol and 1.4 eu, respectively, at the experimental temperature (150−200 °C). The reversibility of the bimolecular butadiene 1,1′ couplings then slows down the rearrangements of the A diradicals, raising the free energies of the product formation paths above the diradical forming TSs and likely above the cycloaddition TSs, too. In other words the faster formation of the diradicals **tt-5** is compensated by their easy dissociation and only a modest fraction of the diradicals can reach the targets.

In an analogous fashion the reversibility of the monomolecular tDVCB opening to the coiled diradicals slows down the rearrangements of the latter and also the simple sequential mechanism of racemization that can be deduced from the shape of the **tt** surface. The sequential mechanism follows the minimal energy path that connects the (*S*,*S*) and (*R*,*R*) DVCB via the coiled conformers. The conformational switches G/A/G− occur without any apparent energetic penalty and with some leakage at the stage of A conformers to form butadiene. The rate of the sequential path decreases because of the reversibility of the steps with an increase of $\Delta G^{\ddagger}$ and the related decrease of $\Delta S^{\ddagger}$ along the path. These features do not fit the experimental results, which demand just the opposite. The results of Hammond and DeBoer place the activation enthalpy and entropy of racemization at 2.3 kcal/mol and 5.8 eu, respectively, above those of the rearrangement implying that the racemization has a higher barrier and lower order than the rearrangement. Note that the rearrangement takes place on the **ct** surface (vide infra) and its rate determining step (TS **15 in-out**) is only 0.4 kcal/mol higher and slightly less ordered than TS **15 out-out**, which serves as the entry into the **tt** surface.

A viable alternative for the racemization is the switch of the initial G conformers to the G− ones by overcoming the butane G/G− barrier **12a** or the higher **12b** (not shown). At first sight this straight path seems unfavorable since TS **12a** is 2.8 kcal/mol above TS **15 out-out**. TS **12a** is, however, less ordered, as demanded by the experimental results, and the rate law for the straight mechanism further improves the entropic balance. Since in this case $k_2 \ll k_{-1}$ the preequilibrium approximation[22] holds and the rate law becomes $k_{\mathrm{obs}} = 2(k_1/k_{-1})k_2$ where factor 2 takes into account the formation of the enantiomeric diradicals which double the racemization rate. Overcoming the **12a** barrier is then the rate-determining step of the straight racemization and factor 2 decreases $\Delta G^{\ddagger}$ by $RT \ln 2$ and increases $\Delta S^{\ddagger}$ by $R \ln 2$ along the path with respect to TS **12a**.

In summary, the **tt** surface offers racemization paths which are somewhat hindered because of either entropic penalties or sizable barriers. The experimental trend is in better accord with the straight racemization than with the sequential one.

The ct Surface: The Stereochemistry of the Rearrangement of DVCB to VCH. The ring opening of the in-out conformers of DVCB t-3 affords an entry into the ct surface. The diradicals can also be accessed from VCH, as shown in Scheme 4. The numbers refer to electronic (free) energies of conformers and TSs relative to aAa **tt-5**. Sequence rules switch the chirality labels in VCH relative to DVCB; to avoid confusion we retain the original capital labels *R* and *S* of DVCB and specify, when needed, the (opposite) VCH chirality with the lower case r and s in brackets.

Ring opening of the optically active (*S*,*S*) DVCB **t-3** leads to the shallow plateau of the chiral coiled DVT **ct-5**

(21) (a) Doering, W. v. E.; Ekmanis, J. L.; Belfield, K. D.; Klärner, F. G.; Krawczyk, B. *J. Am. Chem. Soc.* **2001**, *123*, 5532−5541. (b) Hoffmann, R.; Swaminathan, S.; Odell, B. G.; Gleiter, R. *J. Am. Chem. Soc.* **1970**, *92*, 7091−7098.

(22) (a) Gellene, G. I. *J. Chem. Educ.* **1995**, *72*, 196−9. (b) Carey, F. A.; Sundberg, R. J. *Advanced Organic Chemistry*, 4th ed.; Part A: Structure and Mechanisms; Kluwer Academic/Plenum Publishers: New York, 2000; pp 192−204. (c) See also: Seeman, J. I. *Chem. Rev.* **1983**, *83*, 83−134.

SCHEME 3

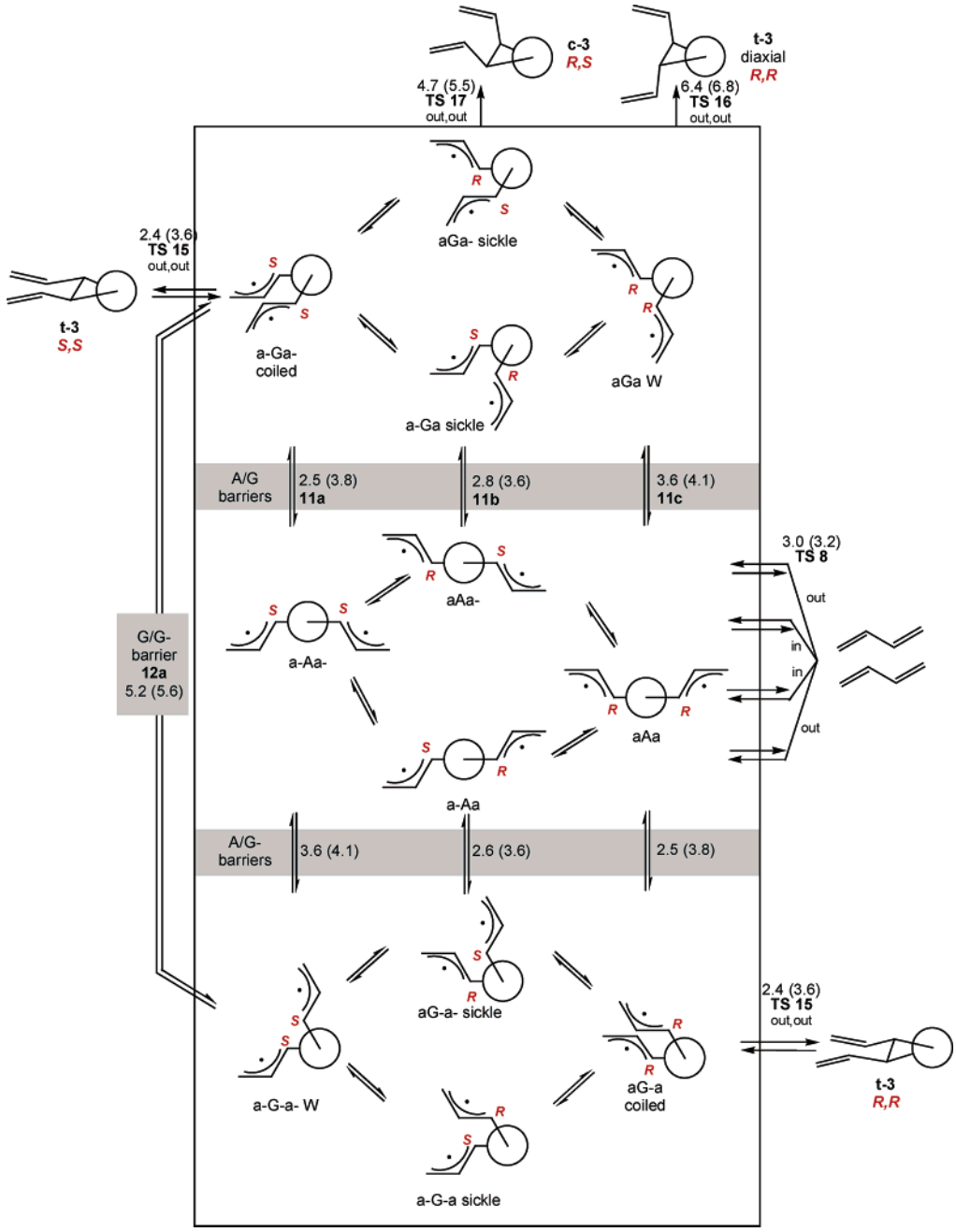

conformer, which equilibrates with the other G conformers. Cyclization to the enantiomers of VCH **2** can occur only from coiled and sickle in conformers. The electronic energies are somewhat misleading in this case since entropy effects make the free energy surface qualitatively and quantitatively different. Cyclization TS **21 tN** is more ordered than the coiled diradical and changes to a saddle on the free energy surface, displaying a higher free energy than that of the cyclization TS **21tX** and the allylic rotation barriers. Due to the $-T\Delta S$ dependence of the free energy this difference increases with increasing temperature and makes the formation of the inverted (*R*) VCH faster than the direct formation of the retained (*S*) VCH. This is in agreement with the experimental results performed at 150−200 °C, where predominant inversion of chirality occurs.

Thermolysis of VCH populates the coiled and sickle in conformers, and the rate-determining step of the VCH racemization is the higher cyclization barrier **21 tN**.

Figure 9 gives the free energy profile related to Scheme 4. The figure clearly points out that the DVCB thermolysis and the VCH racemization take place with distinct high-lying passes with different energetic and thermodynamic characteristics. The red line illustrates the path of the DVCB thermolysis, and the blue line indicates the path of VCH racemization. The paths have much in common (the two diradicals and their rotation barrier as well as the lower **21 tX** cyclization barrier) and differ only for the rate-determining steps, i.e., the cyclobutane opening TS **15 in-out** and the highest cyclization barrier **21 tN**, respectively

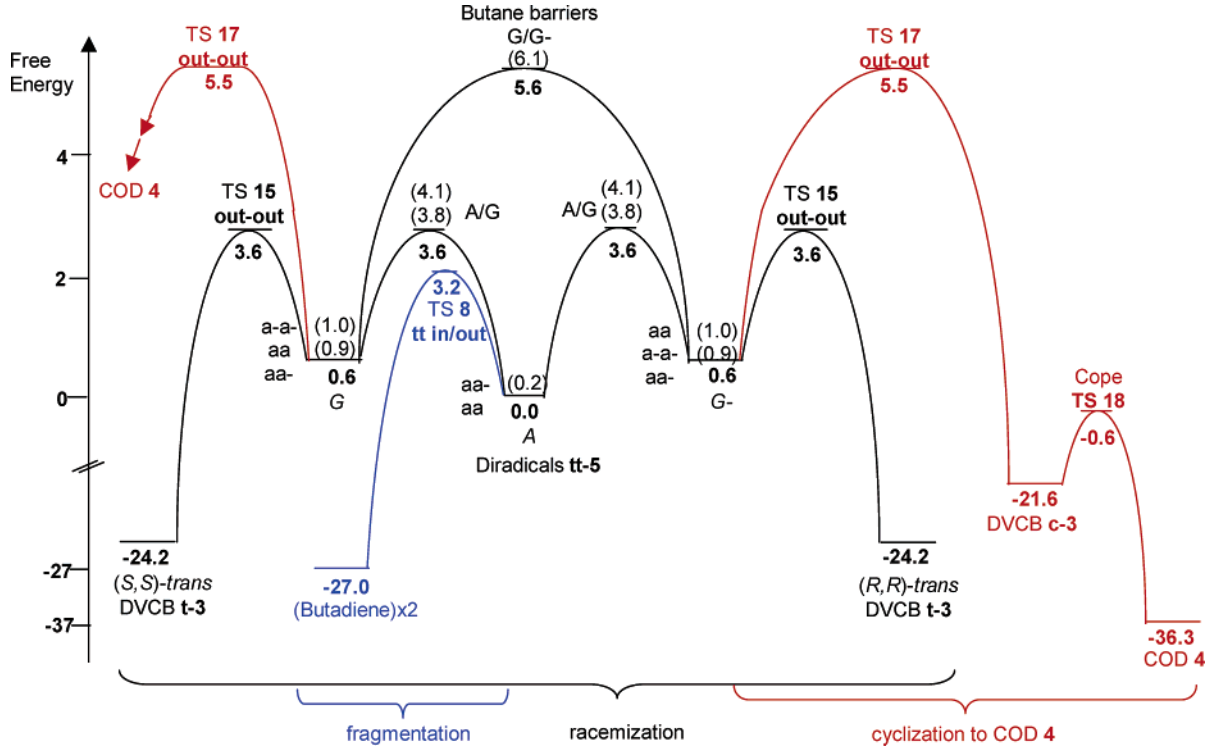

FIGURE 8. Free energy profile of the racemization of (*S*,*S*)-tDVCB and cleavage to butadiene at 298.15 K. Thermolysis of t-DVCB affords initially the coiled conformers **tt-5**. Racemization of (*S*,*S*)-tDVCB requires crossing of the two butane A/G and A/G− barriers or crossing of a single G/G− barrier. Numbers in parentheses indicate other gauche or anti conformers easily attained through the allylic barriers and higher A/G or G/G− barriers. Blue and red lines indicate the connections to butadiene and COD **4**, respectively The easiest pathway of cleavage to two butadienes involves bond breaking of the anti conformers after passage through the A/G barrier.

SCHEME 4

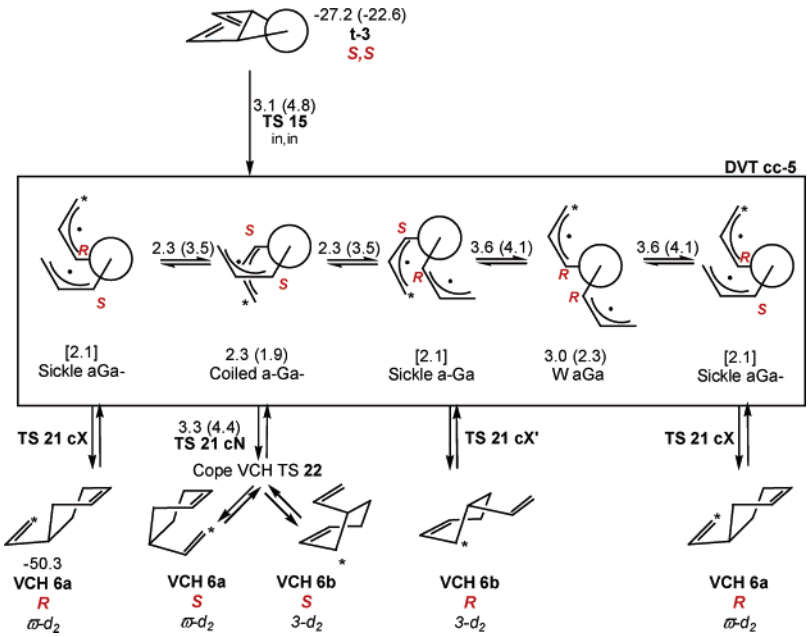

The cc Surface: The VCH Racemization and the d_2 Rearrangement. The diradicals with two cis allyl groups, the so-called **cc** surface, can be formed from DVCB or VCH as shown in Scheme 5 where stars indicate the location of the d_2 labeling of VCH **6a** and **6b** and numbers refer to electronic (free) energies relative to aAa **tt-5**. Here again entropy effects raise sizably the cyclization and rotation barriers.

The **cc** surface offers routes to VCH formation from tDVCB and VCH racemization that are analogous to those described for the lower **ct** surface, where these processes take place more easily. Thus the ring opening

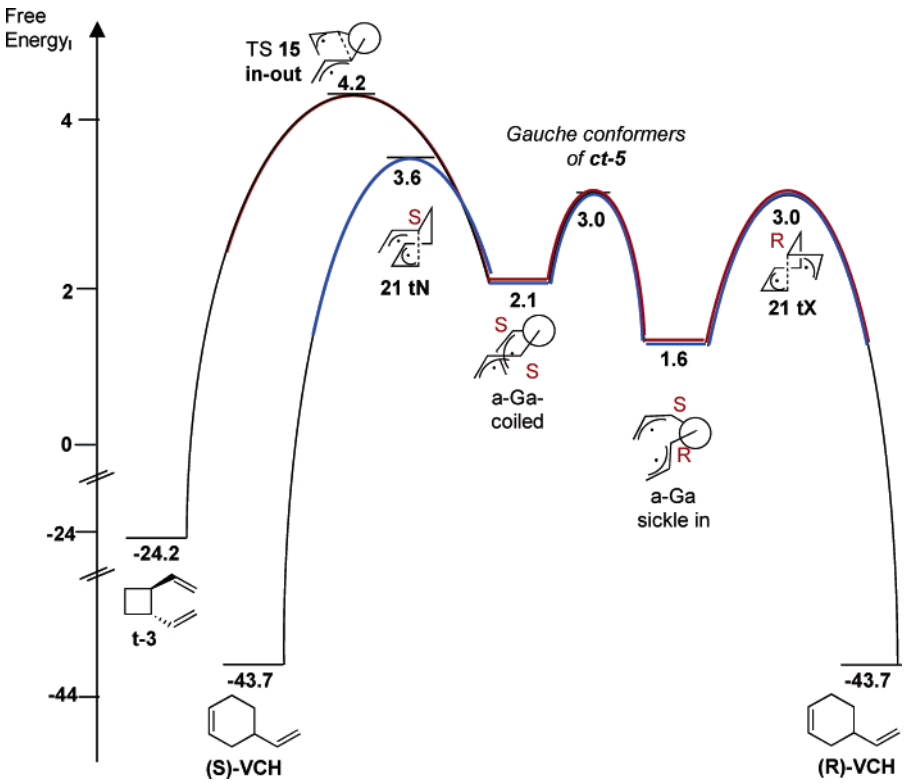

FIGURE 9. Free energy profile at 298.15 K for the t-DVCB thermolysis and VCH racemization on the **ct** surface. The rate determining step in the rearrangement of the (*S*,*S*)-DVCB **t-3 in out** conformer (red path) is the cyclobutane ring cleavage. The product (the major (*R*)-VCH and the minor (*S*)-VCH) determining step involves competition of TS **21 tX** and **21 tN**. In the VCH racemization (blue path) the rate determining step is crossing of the highest cyclization TS **tN**.

SCHEME 5

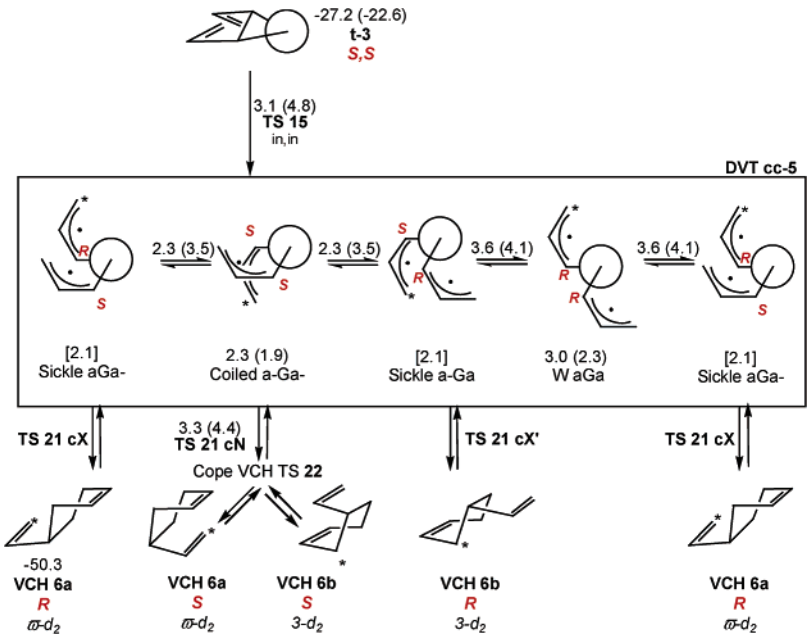

of the **in-in** conformer of (*S*,*S*) DVCB **t-3** affords the chiral coiled DVT **cc-5** conformer, which equilibrates with the sickle aGa− and a-Ga conformers, which are identical in the absence of labeling. The sickle conformers are inherently unstable to cyclization leading to the inverted (*R*) VCH **2** without barriers. Cyclization of the coiled conformer with retention to (*S*) VCH can take place via the floppy TSs **21 cN**, but this cyclization is difficult because of its higher barrier. In an analogous fashion the opening of chiral (*S*) VCH populates the chiral coiled conformer, which easily equilibrates with the sickle conformers affording the (*R*) VCH. The rate-limiting step of the racemization is then the crossing of the highest **21 cN** barrier.

The **cc** surface is, however, essential in accounting for the d_2 VCH rearrangement. The d_2 rearrangement of **6a**

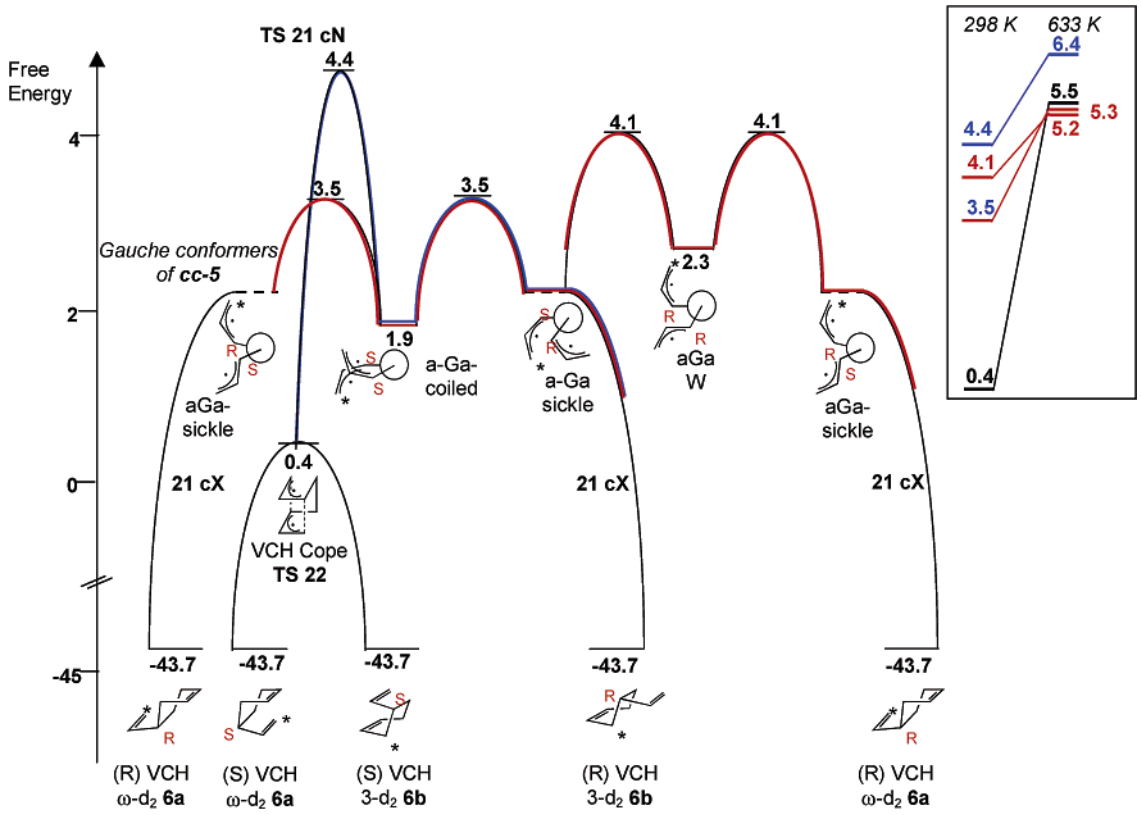

FIGURE 10. Free energy profiles at 298.15 K for the VCH racemization (blue line) and VCH d_2 rearrangement (red lines) on the **cc** surface and the VCH d_2 rearrangement through Cope TS **22** on the ground surface. The inset shows the changes in free energies at the temperature of the experiments (633.15 K, 360 °C). In the VCH racemization the rate-determining step is the cyclization TS **21cN** while in the VCH d_2 rearrangement the rate-determining step involves two twin allylic rotation barriers through the coiled or W conformers. Stars indicate the location of the d_2 labeling of VCH **6a** and **6b**.

to **6b** requires the interconversions of the two sickle aGa− and a-Ga conformers, which can take place through the twin allylic rotations involving the coiled or the W conformer. Note that both the twin paths of d_2 rearrangement avoid the **21 cN** barrier and racemization as well.

Figure 10 displays the free energy profile at 298.15 K of the stepwise diradical VCH racemization (blue line) and d_2 rearrangement (red lines) paths on the **cc** surface, along with the concerted d_2 rearrangement through the VCH Cope TS **22**. Clearly at room temperature the concerted d_2 rearrangement is by far preferred over the stepwise diradical one. However, at the temperature of the experiments (360 °C) the free energy of the VCH Cope TS **22** is raised because of the high order in the Cope TS, which moves above the barriers of the two conformational switches (5.2 and 5.3 kcal/mol) as shown in the inset of Figure 10. Calculations indicate that the mechanism of Doering's d_2 rearrangement depends heavily on the temperature, and that the stepwise diradical mechanism becomes favored over the concerted one at the high temperature of the experiment (360 °C).

For the sake of simplicity we have assumed in the discussion the existence of a sickle **cc-5** diradical intermediate. This sickle diradical may be an entropy-locked intermediate as proposed for tetramethylene by Doubleday.[23]

If no free energy barrier existed for the sickle **cc-5** diradical, the latter would become a fleeting species without a finite lifetime. The paths involving this species and connecting VCH to the coiled and W diradical intermediates could then be regarded as concerted transformations. Figure 11 depicts this situation. The allylic rotation barriers become the TSs for the cyclization steps, and the two remaining diradical intermediates, the coiled and the W diradicals, now have separate identities and different pathways for formation from DVCB and VCH. Since the VCH bond breaking and the allylic rotations are now coupled, the cyclization mode **21 cX** splits into two different cyclization TSs which can be labeled si and ar by using the usual notation of the sigmatropic shifts.[24]

Coupling of bond cleavage and rotation has been described as torquoselectivity.[25] The preference for the si mode in the VCH **21 cX** cleavage avoids repulsive overlap between the σ orbital of the breaking bond and the adjacent cyclohexene π orbital, as suggested for the vinyl cyclopropane rearrangement.[26] For the thermolysis of VCH discussed here, calculations predict a high torquoselectivity in the si mode at 25 °C, but unselective

(23) (a) Doubleday: C. *J. Am. Chem. Soc.* **1993**, *115*, 11968−11983. (b) Doubleday, C. *J. Phys. Chem. A* **2001**, *105*, 6333−6341.

(24) Berson, J. A. *Acc. Chem. Res.* **1968**, *1*, 152−160. Berson, J. A. *Acc. Chem. Res.* **1973**, *5*, 406−414.

(25) (a) Dolbier, W. R., Jr.; Koroniak, H.; Houk, K. N.; Shen, C. *Acc. Chem. Res.* **1996**, *29*, 471−477. (b) Lee, P. S.; Zhang, X.; Houk, K. N. *J. Am. Chem. Soc.* **2003**, *125*, 5072−5079.

(26) (a) Nendel, M.; Sperling, D.; Wiest, O.; Houk, K. N. *J. Org. Chem.* **2000**, *65*, 3259−3268. (b) Baldwin, J. E. *Chem. Rev.* **2003**, *103*, 1197−1212. (c) Leber, P.; Baldwin, J. E. *Acc. Chem. Res.* **2002**, *35*, 279−287.

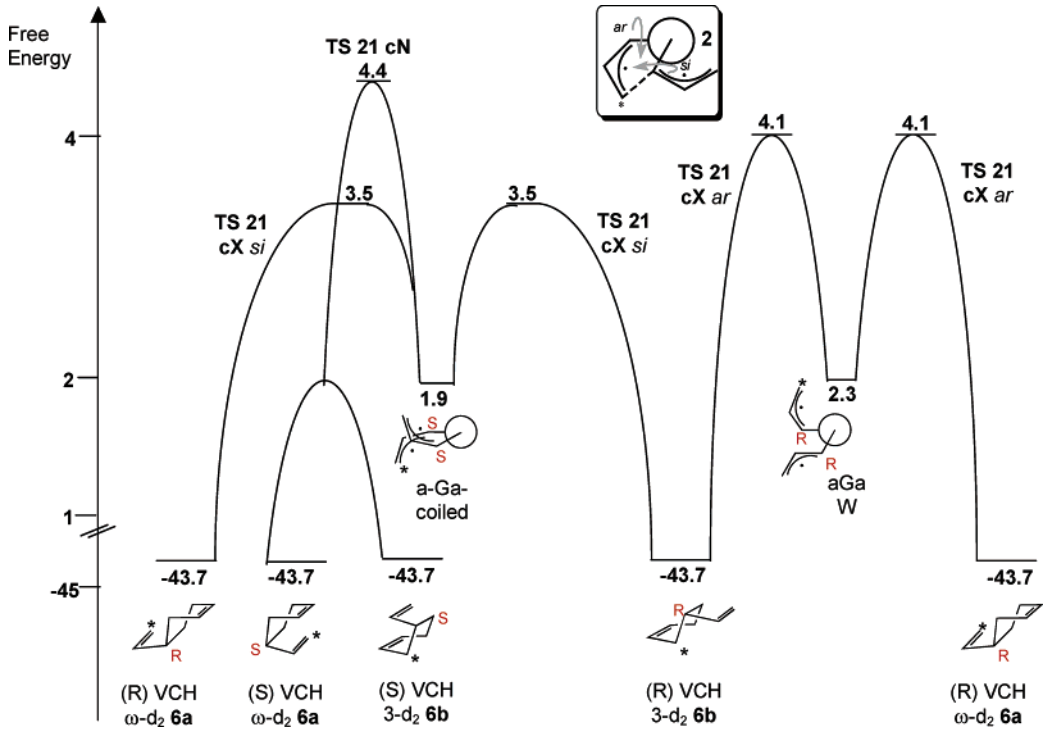

FIGURE 11. Free energy profile of the **cc** surface in the absence of a sickle diradical intermediate. In the thermolysis of VCH the coiled and W diradicals are separately formed and decay in an energetically concerted fashion. Bond breaking and allylic rotations in cleavage of **21 cX** are coupled and give rise to two different TS **21 cX** si and ar, as shown in **25**.

reactions at high temperature due to adverse entropic effects. Dynamic effects such as the Carpenter's dynamic matching[27] may also affect the stereoselectivities. Their detection requires however extensive trajectory calculations.

Comparison with Experimental Activation Parameters. Calculations provide a detailed knowledge of all the elementary steps involved in the interconversions of the various butadiene dimers and allow for the identification of the molecular events, which determine the puzzling experimental activation data (Table 4).

Hammond and DeBoer reported the activation parameters of the DVCB thermolysis[10a] and showed that VCH rearrangement is enthalpically favored and entropically disfavored with respect to the DVCB racemization. Although the calculated activation enthalpies are somewhat lower than the experimental ones, DFT calculations give a similar trend. This is because the VCH rearrangement depends on the DVCB opening TS **15 in-out** while the straight racemization is linked to the butane G/G− barrier **12a**, which has a higher enthalpy but less order. The doubling of the rate in the straight racemization discussed earlier adds a further R ln2 to the activation entropy (with a related decrease of free energy) of the straight path with respect to barrier **12a**.

Doering's results on the VCH thermolysis show that VCH racemization is enthalpically favored and entropically disfavored with respect to the d_2 rearrangement.[9a] The same trend shows up when comparing the lowest cyclization TSs **21 tN** involved in racemization with the d_2 rearrangement TSs, i.e., the less ordered allylic rotation barriers which serve as cyclization TSs **21 cX** si and ar of the coiled and W **cc-5** diradicals, respectively. Calculations presumably overestimate the stability of the VCH Cope TS **22**, which gives the worst fit with the d_2 rearrangement and may not be competitive.

TABLE 4. Experimental and Calculated Thermodynamic Data for the Interconversion of the Butadiene Dimers

path (surface)	$\Delta G^{\ddagger}$	$\Delta H^{\ddagger}$	$\Delta S^{\ddagger}$
DVCB **t-3** thermolysis (175 °C) relative to DVCB **t-3**			
experimental[10a]			
VCH rearrangement		34.0	−1.2
DVCB racemization		36.3	4.6
calculated			
VCH rearrangement, TS **15 in-out** (**ct**)	28.3	28.7	0.9
DVCB racemization, straight (**tt**)	28.4	30.7	4.6
butane G/G− barrier **12a** (**tt**)	29.3	30.7	3.2
VCH thermolysis (360 °C) relative to VCH			
experimental[9a]			
VCH racemization		49.6	−4.7
d_2 rearrangement		52.1	−0.1
calculated			
VCH racemization, TS **21 tN** (**ct**)	45.6	48.7	4.9
d_2 rearrangement, TS **21 cX si** (**cc**)	45.0	50.2	8.2
d_2 rearrangement, TS **21 cX sr** (**cc**)	45.1	48.9	6.0
VCH Cope TS **22**	45.3	42.9	−3.8
butadiene dimerization (175 °C) relative to 2 butadienes			
experimental[28]			
VCH formation		23.5	−29.8
calculated			
DA TS **7 CN**	32.6	22.6	−28.7
DA TS **7 CX**	31.6	22.5	−27.6
diradical TS **tt-8 in** (**tt**)	30.5	23.1	−23.8
diradical TS **tt-8 out** (**tt**)	30.5	23.1	−23.8
butane A/G barrier **11a** (**tt**)	31.7	22.5	−28.1

(27) (a) Carpenter, B. K. *J. Org. Chem.* **1992**, *57*, 4645−4648. (b) Carpenter, B. K. *J. Am. Chem. Soc.* **1995**, *117*, 6336−6344. (c) Carpenter, B. K. *Angew. Chem., Int. Ed.* **1998**, *37*, 3340−3350. (d) Carpenter, B. K. *J. Phys. Org. Chem.* **2003**, *16*, 858−868.

Finally, the calculated thermodynamic data at 175 °C nicely account for the outcome of the butadiene dimerization.[28] The enthalpic barriers of the concerted cycloadditions are similar to the A/G rotational barriers of the anti **tt** diradicals and are lower (by 0.5 kcal/mol) than the diradical forming/breaking TSs. Entropy effects favor remarkably the diradical forming TSs owing to their lesser order and at the experimental temperature the free energy surface shows diradical formation preferred (by 1 kcal/mol) over the concerted cycloadditions. The diradicals dissociate easily and need further energy to overcome the higher rotation barriers to enter into productive channels.

Conclusions

We have explored the undefined and rather mysterious potential energy surface of DVTs where fast internal rotations and interconversions are believed to occur. DFT calculations satisfactorily account for the intriguing behavior of the DVT diradicals and the three calderas **tt-5**, **ct-5**, and **cc-5** provide a rather detailed understanding of their relations to DVCB, VCH, COD, and butadiene.

There is nothing really odd on the surfaces. The enthalpy landscape is smooth due to the easy allylic rotations while entropy effects are larger than usual, because of the relatively high temperature domain used in most experiments.

Aside from the smooth allylic rotation barriers the **tt** surface has normal butane barriers that have to be overcome to effect loss of chirality of DVTs. Straight racemization through the high G/G− barrier is kinetically preferred and this explains the unexpectedly low rate of racemization measured in the experiments of Hammond and DeBoer and Berson. The extraordinary high selectivity in the cleavage of the chiral t-DVCB can be regarded as the origin of the low rate of racemization, since the diradicals are born out exclusively in coiled conformations, which have an unfavorable sequence of reversible steps or high barriers along the racemization paths.

The **ct** surface nicely accounts for the chiral "memory" of the diradical, which mainly cyclizes to inverted VCH, and for the slow VCH racemization, too. The highly selective opening of the chiral t-DVCB places on the **ct** surface a chiral coiled gauche conformer that rotates easily to a sickle gauche conformer. This conformer is prone to cyclize to the inverted VCH through the lowest and less encumbered cyclization barrier. Racemization of chiral VCH requires crossing of the two available cyclization barriers and it is the highest pass which determines the rate.

Finally, the **cc** surface accounts for the highly stereospecific d_2 rearrangement of ω-d_2 VCH **6a** to 3-d_2 VCH **6b**, which involves the twin cyclization TSs **21 cX** si and ar of the coiled and W diradicals.

Aside from clarifying the subtleties of the interconversions of the butadiene dimers, the results provide new insights on the origin of selectivity in the competition between concerted cycloadditions and diradical processes. Although **tt** diradicals form faster than concerted DA cycloadducts, the reversibility of the diradical-forming step in the dimerization of butadiene remarkably decreases the role of the diradical routes to the cyclization products.

Acknowledgment. Financial support by the University of Pavia (FAR), MIUR (PRIN 2002 and 2004), and the National Science Foundation (CHE-9616772 to K.N.H.) is gratefully acknowledged. We also acknowledge CILEA and CINECA for generous allocations of computer time.

Supporting Information Available: Figures showing the conformers of **ct** and **cc** diradicals **5** and the **tt** surface; tables of energetic data of diradicals **5** and their barriers; geometries of all the relevant structures. This material is available free of charge via the Internet at http://pubs.acs.org.

JO0501947

(28) Huybrechts, G.; Luyckx, L.; Vandenboom, T.; Van Mele, B. *Int. J. Chem. Kinet.* **1977**, *9*, 283−293.